J Bionic Eng 15 (2018) 341–355
DOI: https://doi.org/ 10.1007/s42235-018-0026-8

Journal of Bionic Engineering
http://www.springer.com/journal/42235

Multi-Layered CPG for Adaptive Walking of Quadruped Robots

Chengju Liu*, Li Xia, Changzhu Zhang, Qijun Chen

School of Electronics and Information Engineering, *Tongji University*, *Shanghai* 201804, *China*

Abstract

This work concerns biped adaptive walking control on slope terrains with online trajectory generation. In terms of the lack of satisfactory performances of the traditional simplified single-layered Central Pattern Generator (CPG) model in engineering applications where robots face unknown environments and access feedback, this paper presents a Multi-Layered CPG (ML-CPG) model based on a half-center CPG model. The proposed ML-CPG model is used as the underlying low-level controller for a quadruped robot to generate adaptive walking patterns. Rhythm-generation and pattern formation interneurons are modeled to promptly generate motion rhythm and patterns for motion sequence control, while motoneurons are modeled to control the output strength of the joint in real time according to feedback. Referring to the motion control mechanisms of animals, a control structure is built for a quadruped robot. Multi-sensor models abstracted from the neural reflexes of animals are involved in all the layers of neurons through various feedback paths to achieve adaptability as well as the coordinated motion control of a robot's limbs. The simulation experiments verify the effectiveness of the presented ML-CPG and multi-layered reflexes strategy.

Keywords: Multi-Layered CPG (ML-CPG), biological reflex, quadruped robot, adaptive walking

1 Introduction

Depending on nervous systems and sensory feedback, animals can generate stable and adaptive motion in complex and unknown environments. It has been revealed that the rhythmic movements of animals are generated by a series of neural networks called Central Pattern Generators (CPGs)[1,2]. Many attempts at robot motion control in the study of the CPG control mechanism have been made[3–9]. There are two kinds of CPG modeling approaches. One is based on neurons. This kind of model is used to simulate the generation and dynamic behavior of the action potential of a biological neuron action potential. Examples of this kind of model include the H-H model[10,11], the FitzHugh-Nagumo model[12,13], the Morris-Lecar model[14], and the Matsuoka model[15-18] *etc*. This single CPG model based on neurons can generate a rhythmic signal that is like a sine wave. The response of the model to sensing information is to complete an action by adjusting the rhythmic oscillation signal amplitude and cycle. The other modeling approach involves the use of a nonlinear oscillator to model a CPG. The Kuramoto model[19] and the Hopf model[20] are representative examples. Use of a nonlinear oscillator with limit cycle characteristics as the CPG unit is mainly done to research the process of coupling between elements of an overall property. To some extent, these single CPG models can simulate the characteristics of a biological CPG, which partly conform to the response characteristics of a biological neuron. Because the model is relatively simple, it is convenient for use in some engineering applications, such as for snake robot crawling and fish robot swimming[21].

For a biped robot to walk in various ground conditions, the CPG control is primarily based on the simplified single-layered CPG model with some feedback added, which is used to establish the connection relationship between neurons to produce more patterns. However, it also has defects that restrict the effectiveness of its application. The sensing information that is used to adjust the movement is not easy to access. The approach to accessing feedback often involves trial and error. Moreover, the use of feedback information, the response of which to environmental changes is not sufficiently comprehensive and rapid, often yields only an adjustment to the cycle and amplitude of rhythmic movement.

Biologists have found that compared with lower

***Corresponding author:** Chengju Liu
E-mail: liuchengju@tongji.edu.cn

organisms, the CPG neural network structure of reptiles, mammals and other higher animals is more complicated. Therefore, biologists have built different CPG neural network structure models to explain the control mechanism, one of the most famous being the half-center CPG model structure proposed by Brown[22]. Through extending the traditional half-center model, Perret *et al.*[23] set up the two-layered CPG model, which controls the issuance and the intensity of a pulse of motoneurons. Based on the two-layered CPG neural network, Burke[24] introduced sensing information to the middle layer and the motor layer of neurons to realize the layered regulation of motoneuron output. Combined with the CPG interactive control and robot multi-joint coordinated control, Sun *et al.*[25] studied a two-level CPG control mechanism to coordinate the drivers of robot joint, while various feedback information are introduced into the control mechanism. Manoonpong *et al.*[26] designed a hierarchical neural network that included the CPG model to control the leg movement of a robot. Noble *et al.*[27] designed a joint model controlled by a pair of antagonist muscles that can change their angle and stiffness independently. The control system is a multi-layered CPG, each layer of which adopts the H-H neuron model. The connection weights between neurons are adjusted by learning. Nassour *et al.*[28] studied the multimode CPG model and implemented the adaptive motion control of a humanoid robot. Mcrea *et al.*[29] carried out supplementation and correction of the traditional half-center model; the multi-level CPG neural network structure model they put forward better reflects the characteristics of biological rhythmic movement.

The main contribution of this paper is to present a layered CPG model that can generate different motion patterns by altering only several model parameters. The presented ML-CPG model can offer a wide variety of rhythms, patterns and different possibilities to control these patterns to produce walking behaviors. Multiple biological reflex models are established and interact with the ML-CPG. Each reflex is adapted to different layers of the architecture according to the corresponding function complexity and real-time requirements. Moreover, reflex modules are isolated from each other. The proposed CPG model is validated through simulations of a quadrupedal robot.

The rest of this paper is organized as follows. Section **2** describes the ML-CPG model in detail. Section **3** details the entire locomotion control architecture for a quadrupedal robot. The stability of the proposed model for walking on a flat terrain and its adaptation in reaction to an external unknown slope is verified in section **4**. Section **5** gives the conclusion and discussion of the proposed model.

2 Modeling of ML-CPG

2.1 Neural oscillator-based trajectory generators

In this work, based on Rybak's[29,30] work on the two-level CPG model, the basic CPG diagram for one robot joint is proposed in this work as Fig. 1 shows.

The proposed ML-CPG architecture consists of three layers: (i) Rhythm-Generation neurons (RG); (ii) Pattern-Formation neurons (PF); and (iii) motoneurons (MN). In the rhythm-generation layer, rhythmic signals are generated, and its parameters can be modulated easily. In the pattern-formation layer, modulation signals of the movement patterns are generated to determine the different motion modes of controlled objects. Under the control of motion mode commands, the motoneuron layer can calculate and control the controlled object to generate specified trajectories according to the feedback information. The three layers can be regarded as an open structure with access ports in-between, as well as regulatory information from the top. Because the sensory feedback modulates the movement of the layered CPG neurons, the controlled object, the environment and the

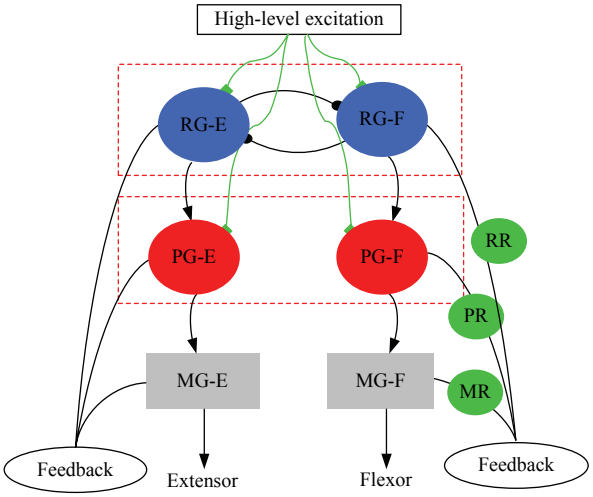

Fig. 1 Multi-layered CPG model for one joint.

CPG controller can constitute a closed-loop control system.

2.2 Interneurons network model

2.2.1 Neural model

The Hopfield continuous neuron model[30] is used to construct interneurons, the equation is as:

$$\begin{cases} \tau_i \dfrac{\mathrm{d}y_i}{\mathrm{d}t} = -\dfrac{y_i}{R_i} + \sum \omega_{ji}\sigma\left(x_j\right) \\ \sigma\left(x_j\right) = \left(1 + e^{\left(\Theta_j - x_j\right)}\right)^{-1} \end{cases}, \tag{1}$$

where y_i represents the neuron membrane potential, τ_i is a time constant, and R_i is the damping coefficient of neuron conduction. x_j represents the jth feedback that a neuron receives. $\sigma(x_j)$ can be interpreted as the strength of external excitation on the neurons. ω_{ji} is the connection coefficient from the jth neuron to the ith neuron, while Θ_j is the role of the threshold of feedback x_j.

The neuron model can quickly respond to feedback signals that are beyond the neuron threshold value. In a complex environment, robots need to receive a variety of sensing information to generate the corresponding motion control signals. Thus, based on the work of Ref. [25], in this work, dynamical model in Eq. (1) is modified as Eq. (2), which is used to construct the Hopfield neural network.

$$\begin{cases} \tau_i \dfrac{\mathrm{d}y_i}{\mathrm{d}t} = -\dfrac{y_i}{R_i} + \sum\limits_j T_{ji} g\left(y_j\right) + I_i,\ i = 1, \cdots, N \\ I_i = \left(1 + \sum\limits_k e^{k_j\left(\Theta_j - x_j\right)}\right)^{-1} \\ y\left(t_0\right) = y^0 \in R^N \\ u_i = \max\left\{y_i, 0\right\} \end{cases}, \tag{2}$$

where N is the number of neurons, T_{ji} represents the connection coefficient between neurons. The input item of external feedback I_i is a bounded function ranging from 0 to 1. The interaction strength of the jth feedback is k_j. $g(y)$ is an S-function expressed as $g(y) = 1/2(1 + \tanh(2\sigma y))$. y_i and u_i are the intermediate state and final output of the neurons, respectively.

When the sensing information exceeds the threshold Θ_j, I_i rapidly grows and reaches its peak value. At the same time, I_i stimulates the output of neurons to its peak. In this model, the intermediate state of neurons y_i being positive indicates that its drive muscle is active, while it being zero represents the corresponding muscle in a state of inhibition. A negative output of neurons has no practical significance in engineering; therefore, a neuron's final output item is expressed as $u_i = \max\{y_i, 0\}$.

2.2.2 Interneurons network

In this work, a neural network model is developed for a robot joint and simulates a biological joint with extensors and flexors working together to control the movement. The network structure is shown in Fig. 2.

The neural network consists of a rhythm generator and a pattern generator, each of which is connected by via stimulation and inhibition connections. The movement model signals of a joint are output through the receiving and processing of external sensing information. As seen from Eq. (2), when $N = 4$, the dynamic model of the interneurons network is expressed as:

$$\begin{cases} \tau_1 \dfrac{\mathrm{d}y_1}{\mathrm{d}t} = -\dfrac{y_1}{R_1} + T_{12} g_2\left(y_2\right) + I_1 \\ \tau_2 \dfrac{\mathrm{d}y_2}{\mathrm{d}t} = -\dfrac{y_2}{R_2} + T_{21} g_1\left(y_1\right) + I_2 \\ \tau_3 \dfrac{\mathrm{d}y_3}{\mathrm{d}t} = -\dfrac{y_3}{R_3} + T_{31} g_1\left(y_1\right) + T_{32} g_2\left(y_2\right) + T_{34} g_4\left(y_4\right) + I_3 \\ \tau_4 \dfrac{\mathrm{d}y_4}{\mathrm{d}t} = -\dfrac{y_4}{R_4} + T_{42} g_2\left(y_2\right) + T_{41} g_1\left(y_1\right) + T_{43} g_3\left(y_3\right) + I_4 \end{cases}. \tag{3}$$

In Eq. (3), each neuron is connected to another neuron of the same layer through inhibiting connections,

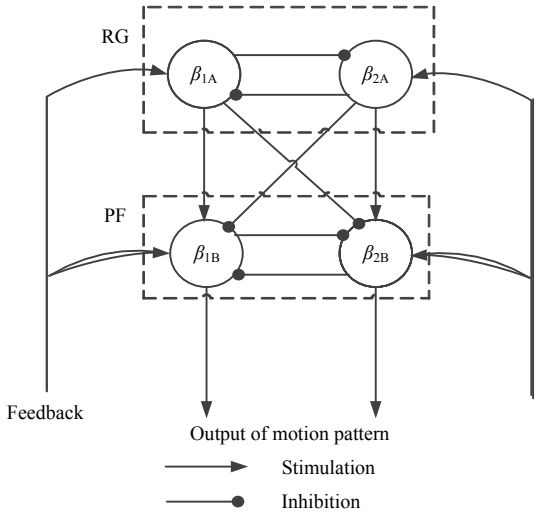

Fig. 2 Structure of interneurons network.

while the different layers are connected through stimulating connections. Set the absolute values of the connection weights equal, and set the neural network connection matrix as:

$$\boldsymbol{T}_{ij} = \begin{vmatrix} 0 & -1 & 0 & 0 \\ -1 & 0 & 0 & 0 \\ 1 & -1 & 0 & -1 \\ -1 & 1 & -1 & 0 \end{vmatrix}. \tag{4}$$

Analyze the stability of the neural network and set matrix $\boldsymbol{W}$ as:

$$\boldsymbol{W} = \frac{\boldsymbol{T}_{ij} + \boldsymbol{T}_{ij}^{\tau}}{2}. \tag{5}$$

If $\mu_{\max}$ is the maximum value of eigenvalues of matrix W, then there exists the following theorem.

According to Theorem in Ref. [31]: Assume that the derivative of each activation function is positive and bounded, for all $x \in R^1$, if $0 < g_i'(x) \le \sigma_i$, and

$$\mu_{\max} < \frac{1}{R_i \sigma_i}, \tag{6}$$

where $\sigma_i > 0$, $i = 1, \cdots, N$, σ_i being the maximum value of $g_i'(x)$, then the neural network Eq. (3), the connection matrix of which is Eq. (4), has one and only one equilibrium point.

Obtain $\mu_{\max} = 2$ through calculating the eigenvalues of matrix $\boldsymbol{W}$; then, when the range of parameters is satisfied, with $R_i\sigma_i < 0.5$, the neural network has one and only one equilibrium point. This is a reference to the parameters selection at the construction of interneurons network to guarantee its stability.

2.2.3 Output of interneurons network

Biological walking involves repeated periodic motion. Thus, in actual control, the interneurons network mainly needs to respond to periodic sensor information. Here, considers the sine signal as an example, the response of a rhythm generator is shown in Fig. 3. The neurons β_{1A} and β_{2A} receive periodic external feedback x_{iA}, and their output is the rhythmic signal u_{iA}. The amplitude of the sine signal x_{iA} is $A_{mp} = 20$, while its period is $T = 2\pi$. The parameters of the rhythm generator are selected as $\tau_{1A} = \tau_{2A} = 0.1$, $R_{1A} = R_{2A} = 1$, and $\sigma_{1A} = \sigma_{2A} = 80$.

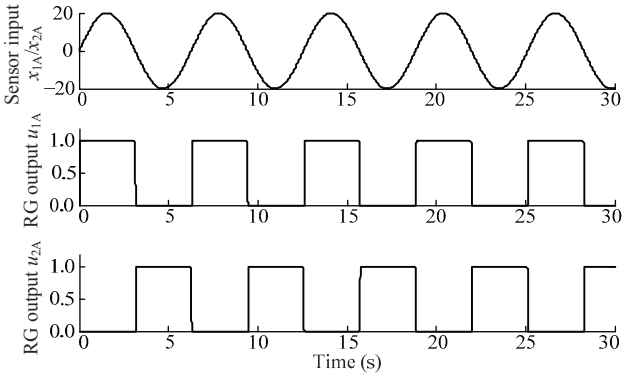

Fig. 3 Response of a rhythmic generator to a periodic signal.

As Fig. 3 shows, a rhythm generator can respond to feedback that exceeds a threshold. The output signal also possesses the states of excitement and inhibition and the characteristics of the outbreak and platform. The two output signals of neurons inhibit each other, which can be used to control the periodic contraction movements of extensors and flexors. The response of a pattern generator to the periodic input signal, which is expressed as follows, is further investigated.

The neurons β_{1B} and β_{2B} receive periodic external feedback x_{iB}. Under the control of the rhythmic generator u_{iA}, the pattern formation outputs the model signal u_{iB}. The amplitude of the sine signal x_{iB} is $A_{mp} = 20$, while its period is $T = \pi$. To distinguish the output of neurons β_{1B} and β_{2B}, the initial phases of x_{1B} and x_{2B} are set to 0 rad and −1.2 rad, respectively. The parameters of the pattern generator are selected as $\tau_{1A} = \tau_{2A} = 0.1$, $R_{1A} = R_{2A} = 1$, and $\sigma_{1A} = \sigma_{2A} = 80$. As Fig. 4 shows, a pattern generator can also respond to feedback that exceeds the threshold under the stimulus of the output signals of upper neurons. To cope with various sensing information, a pattern generator can output different amplitudes of the signals to express different forms of motion.

2.3 Motoneurons model

A single robot joint is considered on the basis of the interneurons network established in Fig. 5. The interaction of a robot with its environment and the dynamics analysis is not considered.

The single robot joint is treated as a second-order spring-damper system. The dynamic system can be described as follows with the parameters: damping coefficient being $b_e = b_f = b$ and elastic coefficient being

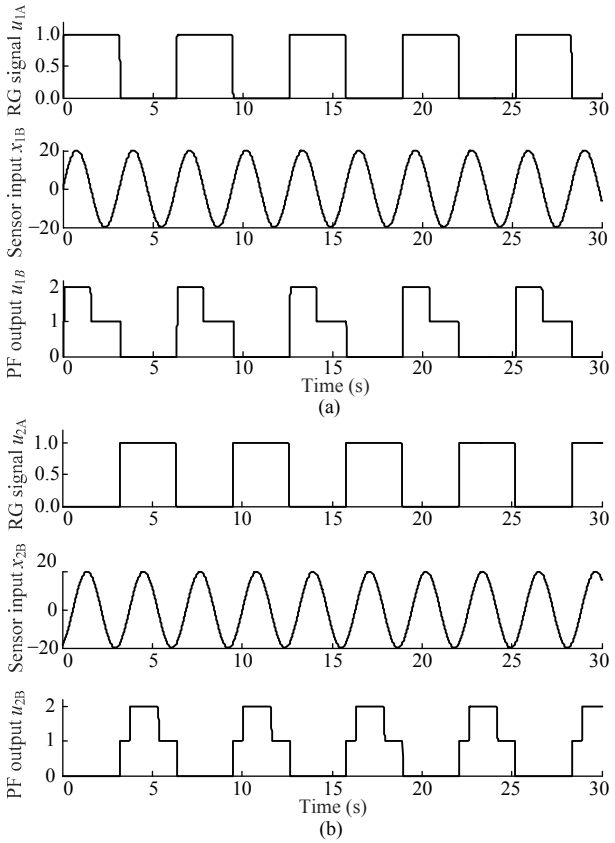

Fig. 4 Response of pattern generators to a periodic signal. (a) Response of pattern generator β_{1B}; (b) response of pattern generator β_{2B}.

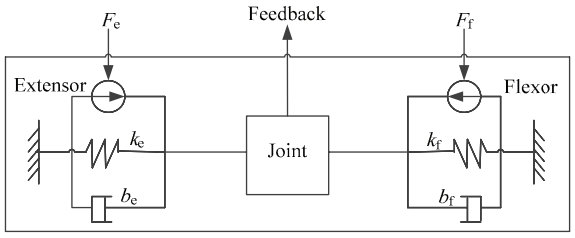

Fig. 5 Engineering model of movement formation.

$k_e = k_f = k$. The transfer function of this second-order spring-damper system is:

$$H(s) = X(s) / F(s) = \frac{1}{ms^2 + bs + k}. \tag{7}$$

Proportional differential control is implemented in this system, and the transfer function of the controller is:

$$G_c(s) = K_p(1 + T_d s). \tag{8}$$

In the actual control of a robot, the execution of different commands results in different transfer functions in each joint. The sensory information that

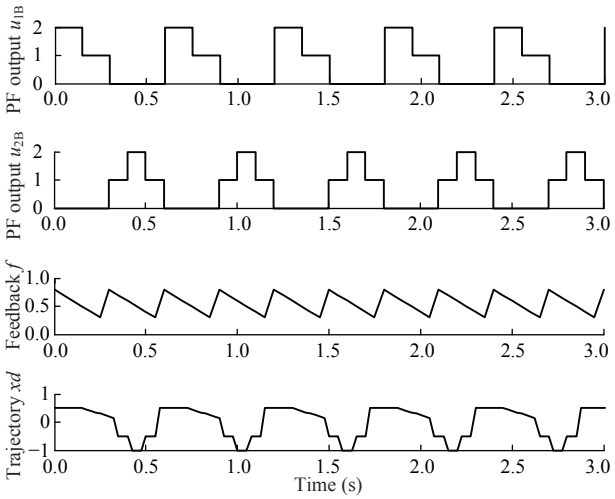

Fig. 6 Output of the motoneurons.

motoneurons receive and the transfer functions will be analyzed and built based on the robot movement process.

The transfer function $H(s)$ of the system is set as Eq. (8), assuming that $m = 2$, $b = 5$ and $k = 1$. Then, the motoneurons are stimulated using the pattern signals in Fig. 4 and the coefficients of proportion and differential control are taken as $k_p = 600$, $T_d = 50$, respectively, to investigate the response output of the motoneurons. Let u_{1B} and u_{2B} be the output of the pattern generators corresponding to the extensor and flexor, respectively, f be the external feedback, the period of which is the same as that of the pattern signals. When the output of u_{1B} and u_{2B} is non-zero, the corresponding muscle is active. Under such a condition, the muscle receives external feedback and generates different movement models according to different pattern signals. Set the expressions of the outputs $F_1(u)$ and $F_2(u)$ of the motoneurons as:

$$\begin{cases} F_1(u) = \begin{cases} 0.8k_1u_{1B} & (1 < u_{1B} \le 2) \\ 0.5 + 0.2f & (u_{1B} \le 1) \end{cases} \\ F_2(u) = \begin{cases} -0.4k_2u_{2B} + 0.2f & (1 < u_{2B} \le 2) \\ -1.2k_2u_{2B} & (u_{2B} \le 1) \end{cases} \end{cases}. \tag{9}$$

The response of the motoneurons is shown in Fig. 6. In Fig. 6, the first two curves are pattern signals of the interneurons network, and the third f is external feedback that the motoneurons receive.

The final curve x_d is the actual response of the spring-damper system, with some delay due to the out-

break and attenuation of pattern signals. Observing the curve x_d reveals that the speed and form of system movement both change periodically with the rhythmical variation of the movement pattern and the feedback information. This indicates that under the activation of pattern signals, the motoneurons can respond in real time, calculate the target trajectory online according to the sensing information, and then, control the system responding quickly to close to the target value.

3 ML-CPG for quadrupedal robot

3.1 Structure of the robot platform

A quadrupedal robot is used as the research platform for verifying the presented ML-CPG motion control method. As Fig. 7 shows, each leg has two initiative joints: hip and knee. The robot has dimensions of 560 mm × 200 mm × 300 mm, excluding the head, while the length of each femur and tibia is 140 mm. The mass of the whole robot is 7.2 kg.

The robot is equipped with the following sensors: GPS, an accelerometer and a gyroscope, which are set on the trunk. The GPS can obtain information from the controller program regarding its absolute position. The accelerometer node measures the acceleration and gravity induced reaction forces over 1, 2 or 3 axes, and it can be used to detect a fall, the up/down direction, *etc*. The gyroscope is used to acquire the inclination of the body. More scrupulously, position sensors, which can obtain the values of all positions and angles, are placed in each joint.

3.2 ML-CPG interactive control structure

3.2.1 Single-legged CPG control structure

Based on the ML-CPG neural network of one joint, the control mechanism of single-legged CPG motion is established to extend of the neural network of a single joint. In Fig. 8, the meaning of each shape is identical to that in Fig. 2. This control structure consists of a rhythm generator, pattern formation, motoneurons layer, virtual robot muscles, and feedback from the interaction between the robot and its environment. The three layers of neurons receive feedback information from the robot itself and the interaction of the robot with its environment. The rhythm generator is composed of two neurons of mutual inhibition, which correspond to the extensor and flexor groups. The pattern formation is composed of four neurons γ_1, γ_2, θ_1 and θ_2, which control the extensor of the hip and the knee and the flexor of the hip and the knee, respectively.

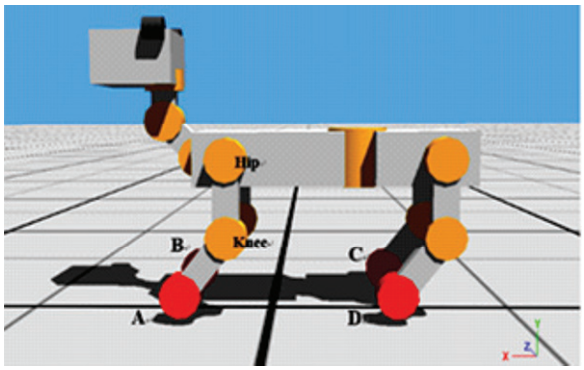

Fig. 7 Screenshot of the quadrupedal robot.

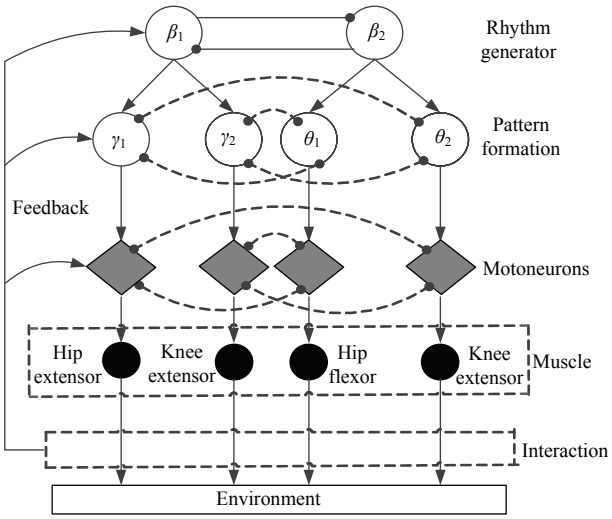

Fig. 8 Structure of the single-legged multilayer CPG interactive control.

In this control network, the lower neurons are completely activated by the upper instructions. Therefore, in the pattern generators and motoneurons, the flexor and extensor neurons do not need inhibitory connections between them to produce the inhibitory output. The inhibition of relations is expressed by the dotted line in the figure.

3.2.2 Four-legged CPG control structure

By merging the four, identical, single-legged CPG control mechanisms and adding stimulating or inhibitory connections between rhythm generators in the same group and the different groups, the four-legged CPG

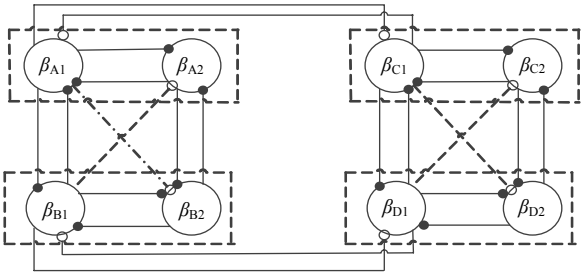

Fig. 9 Connection structure diagram of the rhythm generators.

control structure can be established. The new control mechanism can coordinate the quadrupedal robot to generate a stable walking motion. The connection structure diagram of the four rhythm generators is shown in Fig. 9.

A and B are forelegs, the rhythm generators of which consist of two completely symmetrical parts responsible for the control of A and B. The extensor and flexor are linked by an inhibitory connection. C and D are hind legs, the connection between which is the same as for A and B. Because A and C are in one group during actual movement, the rhythm generators of the extensor are connected by a stimulating connection, the role of which is to coordinate touchdown information and determine the action time of the landing phase. This connection is also used for the B and D group. Furthermore, the pattern generators and motoneurons of each leg are expanded, as shown in Fig. 8. Thus, with the integral control structures of the four legs, the interneurons network of the quadrupedal robot is complete.

On the basis of adding stimulating and inhibitory connections to the four legs of the robot, multi-sensor information is further introduced to the rhythm generators, pattern generators and motoneurons of the control system. Therefore, the two groups of legs can be controlled to alternately generate stable rhythmic movement.

3.2.3 Feedback path of multi-sensor information

Different sensing information is transmitted to all the layers of neurons through different feedback paths. This layered transmission structure can enable a robot system to process multi-sensor information rapidly and in real time. The feedback path is shown in Fig. 10.

The sensor information accessible to the control unit includes the movement state of the robot itself, such as the movement information of the hips and knees, and the interaction state, such as the body angles and joints angles. The introduction principle of the sensor information is as follows: (1) Interneurons receive the sensor information reflecting the interaction state of the robot with its environment. When receiving the upper instructions and the sensing information of the interactive state exceeds the threshold of neurons, the corresponding responses are generated, and the movement instructions are output to activate the lower neurons. Hereinto, the sensing information of pressure under the foot reflects the interaction state of the robot as it contacts the environment; (2) Motoneurons receive the sensor information reflecting the movement state of all parts of the robot and plan the trajectories of muscles in real time. In this sensing information, the position information of hip and knee joints reflects the motion state of the robot. Motoneurons plan the movement trajectory of each muscle in real time according to the body angle and the movement state of the knee and hip joints.

3.2.4 Coordinated motion control method of robot

To realize quadrupedal walking, the four legs of the robot must be coordinated. The coordinated control of robot limbs is realized by changing the motion sequence and intensity of leg joints. Then, the coordination control unit of the robot is established, and the coordination of the robot's limbs is realized by adjusting the input signal and the time delay of neurons. The realization of the action sequence of one robot leg is shown in Fig. 11.

Set the target motion cycle given by the control system as T, and switch the landing foot to the swing phase while the swinging foot is at the moment of touchdown; thus:

$$T = t_{\mathrm{r}} + t_1 + t_2 + t_{\mathrm{f}}, \tag{10}$$

where t_{r} is the time required for a robot leg to lift, which can be determined by planning in advance, t_1 corresponds to the time delay between the rhythm generator and the pattern generator, and t_2 corresponds to the time delay between the pattern generator and the motoneurons. During the execution of stepping forward and falling of a robot leg, the joint that determines the distance from the foot to the ground is mainly the knee. Based on the motion target of the knee and its joint velocity, the

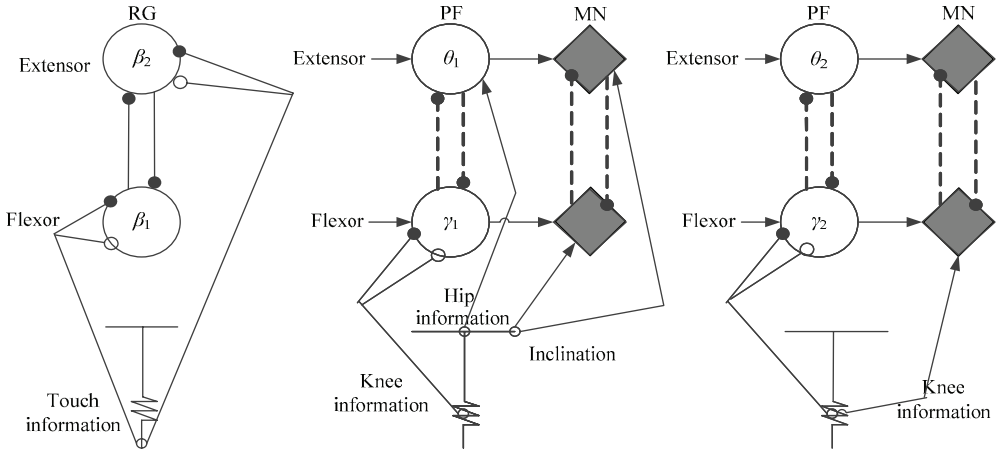

Fig. 10 Multi-sensor information feedback path.

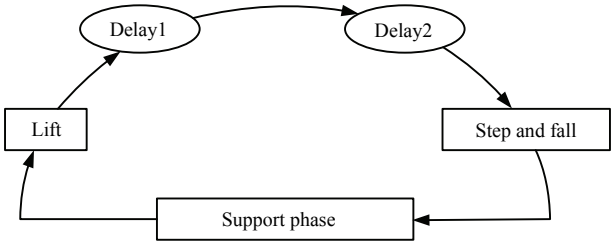

Fig. 11 Robot leg action sequence.

time that passes while a foot falls until achieving touchdown t_f can be estimated based on the delay adjustment, and the control system can adjust the walking cycle to the target value. Then, the stride of the robot can be adjusted automatically by the control system according to the target velocity and target motion cycle.

3.3 Mathematical model of ML-CPG neural network

3.3.1 Mathematical model of interneurons network

An interneurons network must respond to environmental signals rapidly and control muscle motion sequences. First, referring to the connection structure diagram of the rhythm generator shown in Fig. 9, the mathematical model of the rhythm generators of forelegs A and B is expressed as Eq. (11), in which the meanings of parameters τ, y, *etc*., are the same as those in Eq. (2). The subscript β indicates that the layer of that neuron belongs to the rhythm generator, as shown in Fig. 8. In the same way, the equation of the neural network of hind legs C and D is built, the process of which is not repeated here.

Second, the pattern generators of each leg are expanded, as shown in Fig. 8. Here, take the leg A as an example to build the mathematical model (see Eq. (12)), In which, the meanings of parameters τ, y, *etc*., are the same as those in Eq. (2). The subscripts γ, θ indicate that the layer of that neuron belongs to the pattern formation and also represent extensor and flexor, respectively, as well as the subscripts e, f. Moreover, the subscripts H, K represent hip and knee, respectively. In the same way, the equations of the neural networks of the other three legs are built, the processes of which are not repeated here.

3.3.2 Mathematical model of feedback path

According to the multi-sensor information feedback path shown in Fig. 10 and the corresponding principle, and combined with the coordinated control method, the mathematical model of the feedback path is set up. The sensor information added in the control structure is divided into three categories: (1) The interaction between the motoneurons of each joint. In the swing phase, the motoneurons of the knee joint need to integrate their output and the output of the knee joint itself; (2) the interaction between different groups of legs. The swinging legs must adjust the output of joints displacement in real time according to the landing legs and body state, while the landing legs must contract in a timely way and into the oscillating condition according to the state of the swinging legs; (3) sensor information introduced in time delay. The delay of the hip flexor is adjusted based on the position of the knee, and the delay of the knee extensor is adjusted based on the position of the knee.

$$\begin{cases} \tau_{\beta A1}\dfrac{\mathrm{d}y_{\beta A1}}{\mathrm{d}t}=-\dfrac{y_{\beta A1}}{R_{\beta A1}}+T_{A1A2}g_{\beta A2}\left(y_{\beta A2}\right)+T_{A1B1}g_{\beta B1}\left(y_{\beta B1}\right)+T_{A1C1}g_{\beta C1}\left(y_{\beta C1}\right)+I_{\beta A1} \\ \tau_{\beta A2}\dfrac{\mathrm{d}y_{\beta A2}}{\mathrm{d}t}=-\dfrac{y_{\beta A2}}{R_{\beta A2}}+T_{A2A1}g_{\beta A1}\left(y_{\beta A1}\right)+T_{A2B2}g_{\beta B2}\left(y_{\beta B2}\right)+I_{\beta A2} \\ \tau_{\beta B1}\dfrac{\mathrm{d}y_{\beta B1}}{\mathrm{d}t}=-\dfrac{y_{\beta B1}}{R_{\beta B1}}+T_{B1B2}g_{\beta B2}\left(y_{\beta B2}\right)+T_{B2A1}g_{\beta A1}\left(y_{\beta A1}\right)+T_{B1D1}g_{\beta D1}\left(y_{\beta D1}\right)+I_{\beta B1} \\ \tau_{\beta B2}\dfrac{\mathrm{d}y_{\beta B2}}{\mathrm{d}t}=-\dfrac{y_{\beta B2}}{R_{\beta B2}}+T_{B2B1}g_{\beta B1}\left(y_{\beta B1}\right)+T_{B2A2}g_{\beta A2}\left(y_{\beta A2}\right)+I_{\beta B2} \end{cases}. \tag{11}$$

$$\begin{cases} \tau_{\gamma AH}\dfrac{\mathrm{d}y_{\gamma AH}}{\mathrm{d}t}=-\dfrac{y_{\gamma AH}}{R_{\gamma AH}}+T_{AHeA1}g_{\beta A1}\left(y_{\beta A1}\right)+T_{AHeA2}g_{\beta A2}\left(y_{\beta A2}\right)+I_{\gamma AH} \\ \tau_{\theta AH}\dfrac{\mathrm{d}y_{\theta AH}}{\mathrm{d}t}=-\dfrac{y_{\theta AH}}{R_{\theta AH}}+T_{AHfA2}g_{\beta A2}\left(y_{\beta A2}\right)+T_{AHfA1}g_{\beta A1}\left(y_{\beta A1}\right)+I_{\theta AH} \\ \tau_{\gamma AK}\dfrac{\mathrm{d}y_{\gamma AK}}{\mathrm{d}t}=-\dfrac{y_{\gamma AK}}{R_{\gamma AK}}+T_{AKeA1}g_{\beta A1}\left(y_{\beta A1}\right)+T_{AKeA2}g_{\beta A2}\left(y_{\beta A2}\right)+I_{\gamma AK} \\ \tau_{\theta AK}\dfrac{\mathrm{d}y_{\theta AK}}{\mathrm{d}t}=-\dfrac{y_{\theta AK}}{R_{\theta AK}}+T_{AKfA2}g_{\beta A2}\left(y_{\beta A2}\right)+T_{AKfA1}g_{\beta A1}\left(y_{\beta A1}\right)+I_{\theta AK} \end{cases}. \tag{12}$$

The multi-sensor information feedback path is modeled as mathematical equations as well. Here, take leg A as an example to illustrate the sensing information and structure of each neuron.

First, add external feedback adjustment terms $I_{\beta 1}$ and $I_{\beta 2}$ to the rhythm generator neurons β_1 and β_2. The rhythm generator chooses the movement phase after receiving information regarding contact between the feet and the ground. When the contact information is zero, the system determines that the robot is off the ground and switches to the swing phase; when the contact information exceeds a preset threshold, the system determines that robot is in the phase of touchdown. The feedback terms $I_{\beta 1}$, $I_{\beta 2}$ are expressed as:

$$\begin{cases} I_{\beta A1}=\left(1+e^{k_{\beta A1}\left(\Theta_{cA1}-x_{cA}\right)}\right)^{-1} \\ I_{\beta A2}=\left(1+e^{k_{\beta A2}\left(x_{cA}-\Theta_{cA2}\right)}\right)^{-1} \end{cases}, \tag{13}$$

where x_c is the value of contact force between foot and ground, Θ_{ci} is the threshold of sensor information, $k_{\beta i}$ is the interaction strength of feedback. The meanings of the other parameters are the same as those in Eq. (2).

Then, establish external feedback adjustment terms $I_{\gamma H}$, $I_{\theta H}$, $I_{\gamma K}$ and $I_{\theta K}$ in the corresponding pattern generator neurons γ_H, θ_H, γ_K and θ_K, which represent the flexors and extensors of the hip and knee joints, respectively. The pattern generator chooses the movement behavior and sequence after receiving contact information, the joint angle and the output of the rhythm generator. The feedback terms $I_{\gamma H}$, $I_{\theta H}$, $I_{\gamma K}$ and $I_{\theta K}$ are expressed as:

$$\begin{cases} I_{\gamma AH}=\left(1+e^{k_{\gamma AH}\left(\Theta_{\gamma AH}-x_{cA}\cdot x_{cC}\right)}\right)^{-1} \\ I_{\theta AH}=\left(1+e^{k_{\theta AH}\left(\Theta_{\theta AH}-x_{cB}\cdot x_{cD}\right)}\right)^{-1} \\ I_{\gamma AK}=\left(1+e^{k_{\gamma AK}\left(\Theta_{\gamma AK}-x_{cB}\cdot x_{cD}\right)}\right)^{-1} \\ I_{\theta AK}=\left(1+e^{k_{\theta AK}\left(\Theta_{\theta AK}-x_{aA}\right)}\right)^{-1} \end{cases}, \tag{14}$$

where x_a is the value of the knee angle. The meanings of the other parameters are the same as those mentioned above.

Through the establishment of this model structure, a closed-loop control structure is formed among the robot, the ML-CPG neural network, and the environment, which is the foundation for realizing stable, coordinated robot movement in an environment. The

$$F_{\mathrm{AH}(K)\mathrm{e}(f)}=\begin{cases}s_{0\mathrm{H}(K)\mathrm{e}(f)} & (u_{\gamma(\theta)\mathrm{H}(K)}\le 1)\\ \Delta s_{\mathrm{H}(K)\mathrm{e}(f)}+k_{\mathrm{H}(K)\mathrm{e}(f)}\cdot\phi_{\mathrm{pitch}} & (1<u_{\gamma(\theta)\mathrm{H}(K)}\le 2)\end{cases}. \tag{15}$$

feedback sequence embodied in the closed-loop control model is detailed in the next subsection.

3.3.3 Mathematical model of motoneurons

In the interactive control structure of the ML-CPG, the function of the motoneurons is to calculate and output the control torque, velocity or position of the joints in real time according to the sensor information. The input and output can be altered by changing the motion target.

As known from the analysis of the neuron model above, the Hopfield continuous neuron model does not have fixed rhythms and patterns, and it is influenced passively by external sensing information in the determination of the motion sequence of a robot. Therefore, the final output of the model is a kind of timing signal, based on which there are some specific measures that should be taken to control the robot joints. In the current simulation experiments, the appropriate position control is chosen to realize the coordinated movement of the quadrupedal robot.

Here, still take leg A as the example to set the controlled quantity of the flexor and extensor positions for each joint. The generic motoneuron model of the hip extensor is proposed as Eq. (15).

Set $u_{\gamma\mathrm{H}}$ and $u_{\theta\mathrm{H}}$ as the output of the pattern generator corresponding to the hip extensor and flexor. The output value of F_{AHe} and F_{AHf} are both the position signal. s_0 represents the initial position, and Δs represents the target position. Because robot legs A and C are in one group, and B and D are in the other during actual movement, when feet A and C are off the ground, the hip extensor of A is set in initial position, the output of which is zero; the hip flexor of A begins to contract and move towards the target position zero. When feet A and C detect that B and D are off the ground, the hip flexor is set at the initial position. At this time A and C touch the ground, the hip extensor of A begins to stretch and move towards the target position, which is set to kick backward once.

At the same time, the output of the pattern generator corresponding to the knee extensor and flexor the knee are set as $u_{\gamma\mathrm{K}}$ and $u_{\theta\mathrm{K}}$; then, the position signal F_{AKe} and F_{AKf} are the output value. When feet B and D are on the ground, the knee extensor of A begins to move towards the target position, which is set to extend the lengths of the legs. In this way, feet A and C can touch the ground to activate the sequence of feet B and D. In the case of walking uphill and downhill, the target position of the knee extensor needs to be modified according to the torso's pitch angle.

However, when the value exceeds a threshold and the length of the leg is sufficient to touch the ground, the knee flexor begins to shrink and move towards the target position, which is set to shorten the length of the leg to push forward. As with the extensor, the target position of the knee flexor is also modified in the same way. As in the analysis above, here, a whole cycle of the closed loop is completed, and a complete walking cycle of the quadrupedal robot is achieved.

4 Experiment results

To show the effectiveness of the proposed CPG model, two experiments of rhythmic pattern formation presented: walking on a flat terrain and walking on a sloped surface. Webots is used as the platform to process the simulation experiments.

4.1 Gait stability analysis

The parameters used in this experiment are shown in Table 1. With the parameters in Table 1, the robot moves forward on a flat surface with a forward velocity of 0.15 $\mathrm{m\cdot s^{-1}}$, and the gait stability is validated.

Fig. 12 shows snapshots of the walking motion of the quadrupedal robot, depicting 4 representative frames of one cycle. In each pivotal frame, the projection of the robot CoG (Center of Grass) on the ground is within the support polygon, which indicates that the robot can maintain balance of its body during walking.

The phase diagram of the robot torso inclination in three dimensions during a long walking period (240 s, 600 steps) is studied. The three angles of inclination are roll, pitch, and yaw, corresponding to the *y*-*z* plane (*x*-axis), *x*-*y* plane (*z*-axis) and *x*-*z* plane (*y*-axis),

Table 1 Parameters used in the experiment

Parameters	Values
Connection matrix of the rhythm generators A and B $T_{\beta AB}$	$\begin{vmatrix} 0 & -1 & -1 & 0 \\ -1 & 0 & 0 & -1 \\ -1 & 0 & 0 & -1 \\ 0 & -1 & -1 & 0 \end{vmatrix}$
Connection matrix of the pattern generator A $T_{\theta A}$	$\begin{vmatrix} 0 & -1 & 1 & 1 & -1 & -1 \\ -1 & 0 & -1 & -1 & 1 & 1 \\ 0 & 0 & 0 & 0 & 0 & 0 \\ 0 & 0 & 0 & 0 & 0 & 0 \\ 0 & 0 & 0 & 0 & 0 & 0 \\ 0 & 0 & 0 & 0 & 0 & 0 \end{vmatrix}$
Time constant τ_i	0.01
Damping coefficient of neuron conduction R_i	1.00
Parameter of transfer function of neuron σ	80
Interaction strength of jth feedback k_j	10
Threshold of feedback Θ	0 – 1
Initial position of hip joint extensor s_{0He}	0
Target position of hip joint extensor Δs_{He}	−0.3
Initial position of hip joint flexor s_{0Hf}	0
Target position of hip joint flexor Δs_{Hf}	0.3
Initial position of knee joint extensor s_{0Ke}	0
Target position of knee joint extensor Δs_{Ke}	0.5
Initial position of knee joint flexor s_{0Kf}	0
Target position of knee joint flexor Δs_{Kf}	−0.2

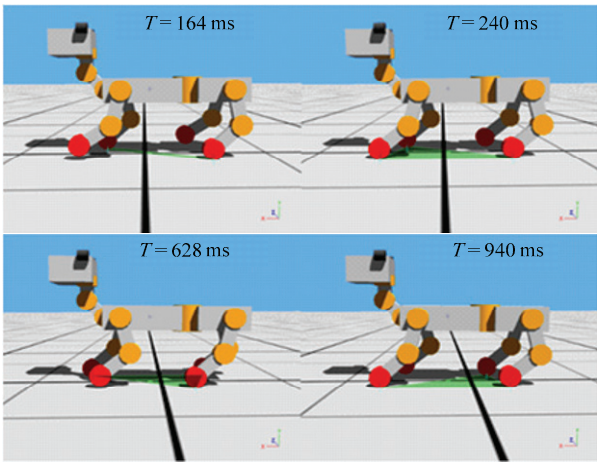

Fig. 12 Simulation images of robot walking on a flat terrain.

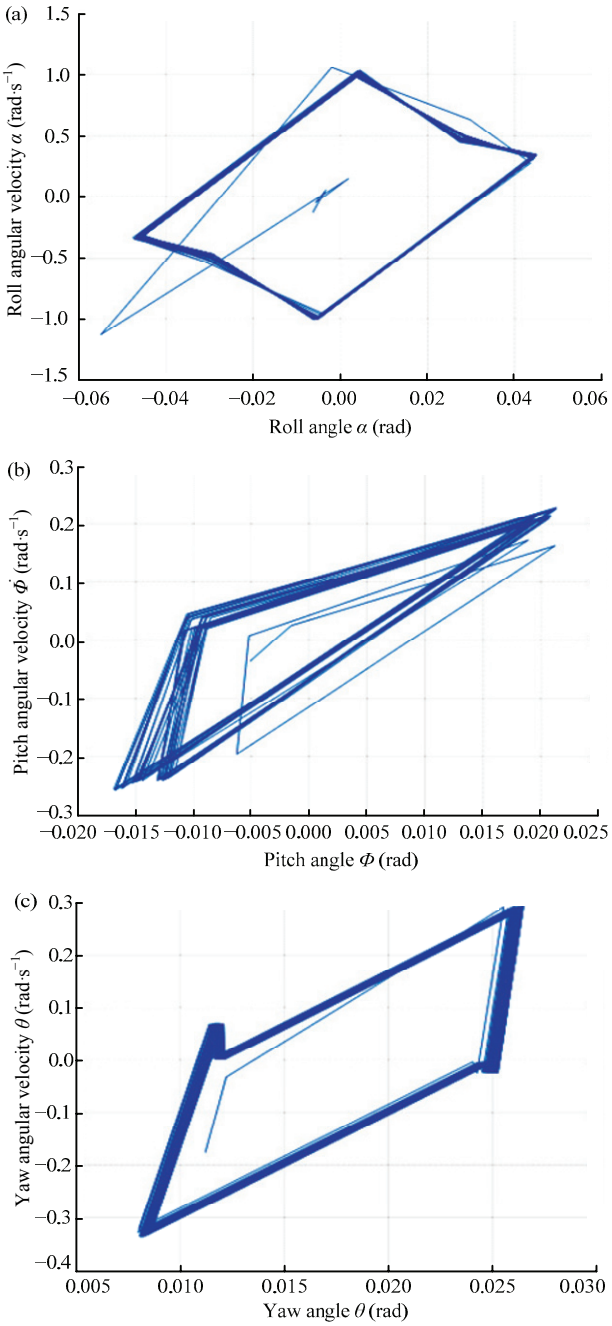

Fig. 13 Trajectories of the robot's movement in the *y*-*z*, *x*-*y*, and *x*-*z* planes. (a) Phase trajectory in *y*-*z* plane; (b) phase trajectory in *x*-*y* plane; (c) phase trajectory in x-z plane.

respectively. The three phase plane trajectories are demonstrated as follows.

Figs. 13a–13c depict trajectories in the phase plane of the robot's movement in the *y*-*z*, *x*-*y* and *x*-*z* planes, respectively. The motion starts from the initial state; therefore, the phase plot starts from the origin point, and then the trajectory spreads out and stays on a stable periodic attractor. The oscillatory movement becomes stable after several steps and converges to a limit cycle, which shows that the gait of the quadrupedal robot is stable and indicates that the control mechanism proposed in this paper can control the quadrupedal robot such that stable movement as the robot interacts with its environment is achieved.

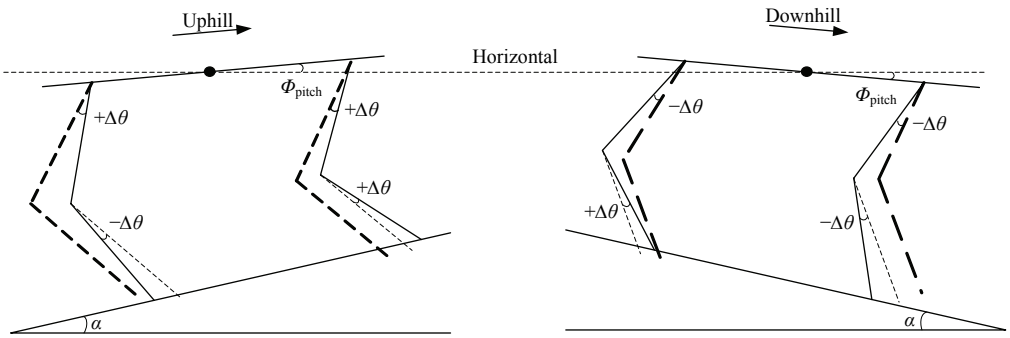

Fig. 14 Postural adjustment of the quadrupedal robot when walking uphill and downhill.

4.2 Adaptation verification

To verify the adaptation of the proposed ML-CPG due to the motoneurons feedback that is used to adjust its parameters, sloped terrain walking is performed. As in the above experiment of walking on a flat terrain, rhythmic patterns are also employed for walking on a sloped terrain; the difference is the postural reflex modeled in the motoneurons.

4.2.1 Postural reflex model

In this work, the postural reflex behavior of animal is imitated and the simulation of a quadrupedal robot is carried out, attempting to make it walk uphill and downhill autonomously. From the observation of animal movement specifically, the postural reflex requires all legs to coordinate with each other harmoniously according to the torso's posture in response to the changing terrain in real time. Therefore, we choose to model this process in the motoneurons layer and design the robot's postural reflex motion to satisfy the following demands: (1) The four legs are required to maintain coordination and obtain an adequate posture by changing the quantity by which they extend or shrink; (2) The forelegs should flex more than the hind legs for uphill walking, while they should flex less than the hind legs for downhill walking to decrease the torso inclination as much as possible.

As shown in Fig. 14, postural adjustment while walking uphill and downhill is clearly demonstrated. The dotted lines are the re-adjusted positions, while the solid lines are the corrected ones. α is the slope angle, which may not equal to the pitch angle of the torso during actual motion. The increment of the positions of the legs $\Delta\theta$, corresponding to the pitch angle ϕ_{pitch} with homologous gains k_{p}, is accessible to the CPG network to adjust the output and generate the control signal with environmental adaptability.

The designed coupling strategy is shown as:

$$\begin{cases} \Delta\theta_{\text{Feed}} = k_{\text{p}} \cdot \phi_{\text{pitch}} \\ \Delta\theta_{\text{Feed}\{e\}} = -\Delta\theta_{\text{Feed}\{f\}} \end{cases}. \tag{16}$$

In the case of walking uphill, a positive angular offset is added to the normal target positions of the foreleg hips, while a negative angular offset is added to the normal target positions of the hips of the hind legs. Similarly, the foreleg knees rotate further, with a positive angular offset to reduce the lengths of the legs. Therefore, the posture of the robot is adjusted to be gentler than the slope inclination and then to maintain the smoothness of motion. Conversely, when walking downhill, the compensations of the hips and knees are automatically opposite those when walking uphill due to the adverse posture. The increment values are acquired based on the inclination of the robot's torso using a built-in inertial unit to implement the function of an accelerometer and a gyroscope.

4.2 Walking uphill and downhill experiment

The slope profile is unknown to the robot. In view of the mechanical structure of the robot, the slope inclination is set to approximately 12°. To verify the effectiveness of the postural reflection, two contrastive experiments (the parameters of the CPG network are the same as for plain walking) are designed.

(1) Experiment 1: Under the condition without postural reflection, when the slope inclination is very small, the robot can walk uphill with a dangerous unsteadiness. However, with the increasing slope inclina-

tion, the phenomenon of slippage often occurs, which ultimately causes the experiment to end in failure. When the robot walks downhill, the capsizing phenomenon occurs as its CoG extends forward.

(2) Experiment 2: With the addition of the proposed postural reflection, the robot can walk through the slope terrain successfully. The experimental results are shown in Figs. 15 and 16.

Based on the characteristic of the postural reflection, access to feedback can change the interaction intensity of the extensor and flexor neurons. Thus, the equilibrium position of the motoneurons output can be offset to adjust the motion of the hips and knees. When walking uphill, the pitch angle is positive, the average of which basically has a linear relationship with the slope, causing the equilibrium position of the curve to move towards the positive direction. Under the action of postural reflection, the output curves of the two front hips and knees gradually move upward because their position offsets continuously increase. Thus, the robot obtains a posture where its head is lower to maintain its balance and to counteract slipping, which is conducive to climbing. As the robot walks on the flat surface, the pitch angle is approximately zero, and each joint is in its initial equilibrium position at the zero line. The trunk of the robot is nearly horizontal. The exact opposite changes to all joints occur in favor of adjusting the robot posture while walking downhill.

The value of the feedback coefficient k_p has great influence on the quality of the robot's ability to walk. If the feedback gain is too large, the offset of the equilibrium position would exceed the peak value of the output signal and result in the output being completely in the positive half of the shaft or negative half of the shaft. In addition, the pitch angle of the robot also has a slight fluctuation when walking on a flat surface. Thus, an overly large feedback gain would amplify the influence of this fluctuation on the CPG output and then aggravate the stability of the robot's horizontal walking ability. Inversely, a gain that is too small would result in the external feedback having little effect on the CPG output, which has no equivalent postural reflection adjustment. The effective experimental range of the feedback coefficient k_p is [0.2, 0.6].

Fig. 17 shows snapshots of the quadrupedal robot walking over the slope. The robot can walk uphill, downhill and transition smoothly with the adjustment of the feedback signal.

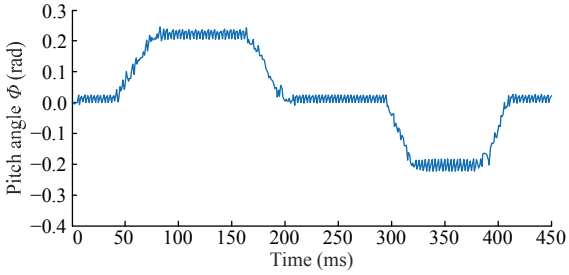

Fig. 15 Pitch angle during slope terrain walking.

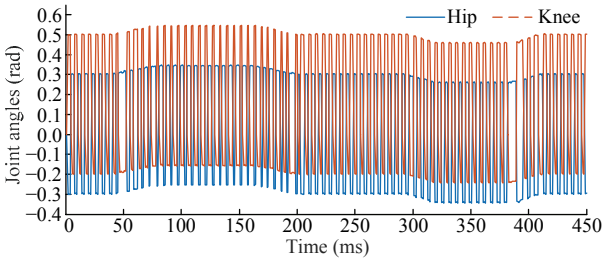

Fig. 16 Control signal of joint angles on slope.

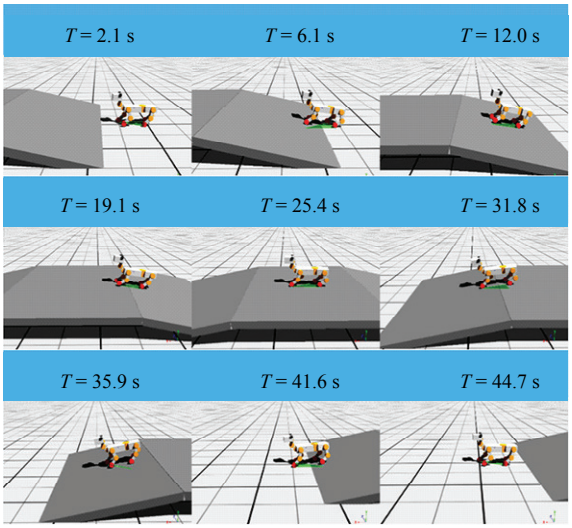

Fig. 17 Quadrupedal robot walking uphill and downhill.

5 Conclusion

This paper proposes ML-CPG based on three layers: rhythm generation, pattern formation, and motoneurons with corresponding feedback access. The effectiveness of the proposed CPG model is verified using a quadrupedal robot. The movement of a quadrupedal robot that involves the interaction of the robot with its environment,

the coordination of joints and limbs, and the expansion of the ML-CPG is specifically analyzed. The gait stability of the proposed model is obtained for the case of walking on a flat terrain, with its phase trajectories possessing a near periodic orbit. Imitating the characteristics of the vestibular reflection of animals, the postural reflection mechanism of a quadrupedal robot for slope movement is modeled, which offsets the equilibrium position of the control signal to adjust the robot's posture. The results show that the quadrupedal robot can walk uphill and downhill.

Further work will involve experiments on a real quadrupedal and biped robot, which will have a stronger impact on the control mechanism. Furthermore, the imitation of biological reflex actions and a control model with multi-jointed legs are worth researching in depth.

Acknowledgment

This work was supported by the National Natural Science Foundation of China (Grant Nos. U1713211 and 61673300)).

References

[1] Beer R D, Chiel H J, Gallagher J C. Evolution and analysis of model CPGs for walking: II. General principles and individual variability. *Journal of Computational Neuroscience*, 1999, **7**, 119–147.

[2] Hooper S L. Central pattern generators. *Current Biology*, 2000, **10**, R176–R177.

[3] Wu Q D, Liu C J, Zhang J Q, Chen Q J. Survey of locomotion control of legged robots inspired by biological concept. *Science in China Series F*: *Information Sciences*, 2009, **52**, 1715–1729.

[4] Liu C, Chen Q, Wang D. CPG-inspired workspace trajectory generation and adaptive locomotion control for quadruped robots. *IEEE Transactions on Systems*, *Man*, *and Cybernetics*, *Part B* (*Cybernetics*), 2011, **41**, 867–880.

[5] Liu C, Wang D, Chen Q. Central pattern generator inspired control for adaptive walking of biped robots. *IEEE Transactions on Systems*, *Man*, *and Cybernetics*: *Systems*, 2013, **43**, 1206–1215.

[6] Zhong G L, Chen L, Jiao Z D, Deng H. Locomotion control and gait planning of a novel hexapod robot using biomimetic neurons. *IEEE Transactions on Control Systems Technology*, 2018, **26**, 624–636.

[7] Yang K. Dynamic model and CPG network generation of the underwater self-reconfigurable robot. *Advanced Robotics*, 2016, **30**, 925–937.

[8] Liu C, Wang D, Goodman E D, Chen Q J. Adaptive walking control of biped robots using online trajectory generation method based on neural oscillators. *Journal of Bionic Engineering*, 2016, **13**, 572–584.

[9] Yu J, Wu Z, Wang M, Tan M. CPG network optimization for a biomimetic robotic fish via PSO. *IEEE Transactions on Neural Networks and Learning Systems*, 2016, **27**, 1962–1968.

[10] Hodgkin A L, Huxley A F. Currents carried by sodium and potassium ions through the membrane of the giant axon of Loligo. *Journal of Physiology*, 1952, **116**, 449–472.

[11] Wang H, Yu Y G, Wang S, Yu J. Bifurcation analysis of a two-dimensional simplified Hodgkin–Huxley model exposed to external electric fields. *Neural Computing and Applications*, 2014, **24**, 37–44.

[12] FitzHugh R. Impulses and physiological state in theoretical models of nerve membrane. *Biophysical Journal*, 1961, **1**, 445–466.

[13] Nagumo J, Arimoto S, Yoshizawa S. An active pulse transmission line simulating nerve axon. *Proceedings of the IRE*, 1962, **50**, 2061–2070.

[14] Morris C, Lecar H. Voltage oscillations in the barnacle giant muscle fiber. *Biophysical Journal*, 1981, **35**, 193–213.

[15] Matsuoka K. Mechanism of frequency and pattern control in the neural rhythm generators. *Biological Cybernetics*, 1987, **56**, 345–353.

[16] Taga G, Yamaguehi Y, Shimizu H. Self-organized control of bipedal locomotion by neural oscillators in unpredictable environment. *Biological Cybernetics*, 1991, **65**, 147–159.

[17] Fukuoka Y, Kimura H. Dynamic locomotion of a biomorphic quadruped 'Tekken' robot using various gaits: Walk, trot, free-gait and bound. *Applied Bionics and Biomechanics*, 2009, **6**, 1–9.

[18] Zhang X L, Mingcheng E, Zeng X Y, Zheng H J. Adaptive walking of a quadrupedal robot based on layered biological reflexes. *Chinese Journal of Mechanical Engineering*, 2012, **25**, 654–664.

[19] Acebrón J A, Bonilla L L, Vicente C J P, Ritort F, Spigler R. The Kuramoto model: A simple paradigm for synchronization phenomena. *Reviews of Modern Physics*, 2005, **77**, 137–185.

[20] Hopfield J J. Neural networks and physical systems with emergent collective computational abilities. *Proceedings of the National Academy of Sciences*, 1982, **79**, 2554–2558.

[21] Manzoor S, Choi Y. A unified neural oscillator model for

various rhythmic locomotions of snake-like robot. *Neurocomputing*, 2016, **173**, 1112–1123.

[22] Brown T G. On the nature of the fundamental activity of the nervous centres; together with an analysis of the conditioning of rhythmic activity in progression, and a theory of the evolution of function in the nervous system. *The Journal of Physiology*, 1914, **48**, 18–46.

[23] Perret C, Cabelguen J M, Orsal D. Analysis of the pattern of activity in "Knee Flexor" motoneurons during locomotion in the cat. In: Gurfinkel V S, Ioffe M E, Massion J, Roll J P, eds., *Stance and Motion*, Springer, Boston, USA, 1988, 133–141.

[24] Burke R E, Degtyarenko A M, Simon E S. Patterns of locomotor drive to motoneurons and last-order interneurons: Clues to the structure of the CPG. *Journal of Neurophysiology*, 2001, **86**, 447–462.

[25] Wang T, Guo W, Li M, Zha F, Sun L. CPG control for biped hopping robot in unpredictable environment. *Journal of Bionic Engineering*, 2012, **9**, 29–38.

[26] Manoonpong P, Pasemann F, Wörgötter F. Sensor-driven neural control for omnidirectional locomotion and versatile reactive behaviors of walking machines. *Robotics and Autonomous Systems*, 2008, **56**, 265–288.

[27] Noble F K, Potgieter J, Xu W L. Modelling and simulations of a central pattern generator controlled, antagonistically actuated limb joint. *IEEE International Conference on Systems*, *Man*, *and Cybernetics* (*SMC*), Anchorage, USA, 2011, 2898–2903.

[28] Nassour J, Hénaff P, Benouezdou F, Cheng G. Multi-layered multi-pattern CPG for adaptive locomotion of humanoid robots. *Biological Cybernetics*, 2014, **108**, 291–303.

[29] McCrea D A, Rybak I A. Organization of mammalian locomotor rhythm and pattern generation. *Brain Research Reviews*, 2008, **57**, 134–146.

[30] Hopfield J J. Neural networks and physical systems with emergent collective computational abilities. *Proceedings of the National Academy of Sciences*, 1982, **79**, 2554–2558.

[31] Yang H, Dillon T. Exponential stability and oscillation of Hopfield graded response neural network. *IEEE Transactions on Neural Networks*, 1994, **5**, 719–729.